TISSUE ENGINEERING: Part C
Volume 15, Number 1, 2009

DOI: 10.1089/ten.tec.2007.0366

Laminin Nanofiber Meshes That Mimic Morphological Properties and Bioactivity of Basement Membranes

Rebekah A. Neal, B.S.,[1] Samuel G. McClugage, III, B.A.,[1] Mia C. Link, B.S.,[1] Lauren S. Sefcik, B.S.,[1] Roy C. Ogle, Ph.D.,[1–4] and Edward A. Botchwey, Ph.D.[1–3,5]

The basement membrane protein, laminin I, has been used broadly as a planar two-dimensional film or in a three-dimensional form as a reconstituted basement membrane gel such as Matrigel to support cellular attachment, growth, and differentiation *in vitro*. In basement membranes *in vivo*, laminin exhibits a fibrillar morphology, highlighting the electrospinning process as an ideal method to recreate such fibrous substrates *in vitro*. Electrospinning was employed to fabricate meshes of murine laminin I nanofibers (LNFs) with fiber size, geometry, and porosity of authentic basement membranes. Purified laminin I was solubilized and electrospun in parametric studies of fiber diameters as a function of polymer solution concentration, collecting distance, and flow rate. Resulting fiber diameters ranged from 90 to 300 nm with mesh morphologies containing beads. Unlike previously described nanofibers (NFs) synthesized from proteins such as collagen, meshes of LNFs retain their structural features when wetted and do not require fixation by chemical crosslinking, which often destroys cell attachment and other biological activity. The LNF meshes maintained their geometry for at least 2 days in culture without chemical crosslinking. PC12 cells extended neurites without nerve growth factor stimulation on LNF substrates. Additionally, LNFs significantly enhance both the rate and quantity of attachment of human adipose stem cells (ASCs) compared to laminin films. ASCs were viable and maintained attachment to LNF meshes in serum-free media for at least 3 days in culture and extended neurite-like processes after 24 h in serum-free media conditions without media additives to induce differentiation. LNF meshes are a novel substrate for cell studies *in vitro*, whose properties may be an excellent scaffold material for delivering cells in tissue engineering applications *in vivo*.

Introduction

The laminins are a family of ubiquitous basement membrane proteins that serve critical functions in cell attachment, growth, migration, and differentiation of many cell types. Laminin I is the first extracellular matrix protein to appear during embryonic development, where it surrounds the inner cell mass of the compacted blastocyst.[1] Studies of laminin I purified from the Engelbreth–Holm–Swarm (EHS) tumor established that laminin is required for cell attachment and growth, and many studies confirm the importance of laminins in development and survival.[2,3] Laminin interacts with cells through a variety of integrins,[4] the dystroglycan receptor,[5] syndecan,[6] and other receptors broadly expressed on many cell types.[7,8]

A fibrous network of laminin alone may retain sufficient conformation reminiscent of basement membrane sufficient to promote cell adhesion and growth. Laminin in the basement membrane actually self-assembles into a fibrous network independent of other basement membrane constituents. Yurchenco *et al.* have demonstrated that laminin forms a polymer network independently of collagen IV in the basement membrane *in vivo*, as well as *in vitro*.[9] While laminin does not require the presence of other polymers to form a fibrous mesh during development, it does regulate the conformation of other basement membrane components. For instance, it can drive incorporation of type IV collagen into a mature basement membrane network, and in fact, Tsiper and Yurchenco have shown that laminin is necessary for collagen to successfully polymerize.[10] Additionally, Flemming *et al.* have shown that purely topographical cues produced by the conformation of the extracellular matrix can guide cell behavior and morphology.[11] As laminin nanofibrous meshes are composed of a major basement membrane constituent and maintain a geometrical conformation similar to *in vivo* basement membrane, a fibrous laminin network may be sufficient to promote cell adhesion and growth in an environment reminiscent of basement membrane.

To create a biomimetic laminin membrane, both the morphology and the composition of the membrane must be

[1]Department of Biomedical Engineering, [2]Department of Medicine, [3]Center for Immunity, Inflammation, and Regeneration, [4]Department of Plastic Surgery, and [5]Department of Orthopaedic Surgery, University of Virginia, Charlottesville, Virginia.

considered.[11] Feature sizes of the human corneal epithelial basement membrane have been measured at 47–380 nm in height with diameters in the range of 22–92 nm,[12] falling within the nanoscale range. In the same study, electron micrographs of the corneal epithelial basement membrane illustrate morphology reminiscent of a hydrated nanofiber (NF) mesh.

Previous efforts to manufacture feature sizes on the nanometer scale have been unsuccessful with traditional printing and etching techniques.[11] Currently, the optimal method for producing fibers of these dimensions is the electrospinning technique. The basic method for electrospinning involves maintaining a polymer solution at its surface tension at the tip of a needle through the use of a syringe pump. When a voltage is applied to the needle, the outer layers of the polymer receive a charge that pulls them out of the needle toward a grounded collector. As the solution leaves the needle, the solvent evaporates, and dry polymer fibers are collected. Electrospinning as a technique is appealing because the physical parameters are easily varied and exert considerable effects on the resulting polymer fiber morphology. While several investigators have successfully fabricated protein NFs in the range of 100–300 nm from interstitial collagens[13] and elastin[14] using electrospinning techniques, we have discovered appropriate parameters to achieve laminin I nanofibers (LNFs) via electrospinning.

If it is to possess the biological properties of a natural basement membrane, the laminin I nanofiber (LNF) mesh should be a favorable substrate for cell attachment and growth in a wide variety of tissue engineering applications. Laminin is particularly relevant for nervous system tissue engineering because laminin has been shown to encourage neurite extension.[15] However, studies demonstrate that the bioactive properties of laminin are fragile and often destroyed by processing methods, such as lyophilization and exposure to ultraviolet light, which are required to form laminin substrates for *in vitro* cell culture studies.[16] Electrospinning typically requires lyophilization of proteins and subsequent solubilization in highly volatile organic solvents to form the initial polymer solution. Other groups have faced this challenge when electrospinning interstitial collagens, and one might expect to encounter similar obstacles with laminin.[17,18] These studies have often shown that electrospun collagen fibers flatten and form a ribbon-like morphology in aqueous medium, decreasing porosity and surface roughness of the substrates.[17,18] Additionally, Zeugolis *et al*. have shown potential for collagen denaturation to gelatin by solubilization in fluoroalcohols such as 1,1,1,3,3,3-hexaflouro-2-propanol (HFP) and subsequent electrospinning.[19] To overcome the issue of fiber flattening in collagen-electrospun matrices, researchers employ chemical crosslinkers such as glutaraldehyde. While glutaraldehyde crosslinking does add some structural stability to the NF matrices, the meshes lose a large percentage of their porosity and surface roughness. In addition, glutaraldehyde is cytotoxic, and may be difficult to entirely remove after crosslinking treatment.[20] Due to the sensitivity of LNFs, glutaraldehyde crosslinking may destroy the bioactivity of the laminin protein.

In this study, our objective was twofold: first, to determine appropriate parameters for creating electrospun LNF meshes that mimic the dimensions and morphology of *in vivo* basement membrane, and second, to confirm that LNF meshes retained bioactivity after fabrication and hydration. We conducted parametric studies in which we varied physical process parameters, and measured changes in fiber morphology by quantifying diameter and bead area density. Additionally, we examined the preservation of laminin bioactivity after processing by measuring attachment and neuronal differentiation of adipose stem cells (ASCs) on LNFs in serum-free culture conditions, and by observing neurite extension of PC12 cells on LNFs with and without the presence of nerve growth factor (NGF).

Materials and Methods

Materials

The solvent HFP was purchased from Sigma (St. Louis, MO). All cell culture reagents were purchased from Fisher Scientific (Pittsburg, PA).

Laminin isolation

Laminin I was purified from the EHS tumor according to previously established methods.[21,22] The final laminin solution was subjected to two rounds of precipitation with 45% ammonium sulfate to remove most growth factors present. Purity of laminin was evaluated by SDS-PAGE and western analysis with affinity-purified antibodies to type IV collagen, entactin/nidogen, and perlecan, the major contaminants of such preparations. Purity was determined to be greater than 99% laminin (w/v). Laminin was stored at −80°C.

Laminin electrospinning

For the parametric study, a series of process parameters was chosen within ranges shown to be successful in creating submicron or nanoscale fibers of other ECM proteins such as collagens[13] and fibrinogen.[23] Laminin was dialyzed exhaustively against dH_2O, lyophilized, and dissolved overnight with stirring at 4°C in HFP to achieve desired concentrations prior to electrospinning: 3%, 5%, or 8% (w/v) final solution. The laminin solution was loaded into a 5 mL glass syringe with an 18G blunt needle, and mounted into an Aladdin programmable syringe pump (World Precision Instruments, Sarasota, FL). A collector plate covered with aluminum foil was placed 12.5 or 25 cm below the tip of the needle and electrically grounded. A high-voltage power supply (Gamma, Ormond Beach, FL) was connected with the positive lead on the needle and set at 20 kV. The syringe pump was programmed to dispense the solution at 0.5, 1.5, 2.0, or 3.0 mL/h. Laminin was allowed to collect on the aluminum foil for at least 20 min before the sample was removed and the parameters changed. Samples were cut from the aluminum foil, mounted on aluminum stubs (Electron Microscopy Sciences, Hatfield, PA), sputter coated with gold using a BAL-TEC SCD005 sputter coater, and imaged using a JEOL JSM6400 scanning electron microscope (SEM) with Orion image processing at 15 kV accelerating voltage and 39-mm working distance.

Fiber diameter and bead area density analysis

Scanning electron micrographs taken on a JEOL 6400 SEM with Orion image processing were analyzed for fiber diameter using Image J (open source program available from NIH). For

fiber diameter measurements, we followed protocols previously described by our group[24] and others.[25] Briefly, images were opened in Image J, and the measure tool was used to find the average diameter of at least 50 fibers per sample, with at least four samples per condition. Bead area density was determined by finding the average diameter of each bead and calculating the area based on the assumption that all beads were roughly circular in shape. The threshold function in Image J was used to change the image to black-and-white pixels, and the total surface area of laminin was measured, including fibers and beads. This total area divided by the already-calculated bead area yielded the bead area density per sample. Each bead with a diameter larger than twice the average fiber diameter was counted in each sample, and at least four sample images were used per condition. For both fiber diameter and bead area density, a minimum of three samples were used with a minimum of 50 measurements made per sample, and error bars indicate standard error.

Laminin scaffold and film preparation for cell culture

To prepare LNF scaffolds for cell culture, 12-mm-diameter round coverslip glass was surface charged using the Lectro-Treat 3D Surface Treater (Lectro Engineering, St. Louis, MO) and placed on the grounded collector opposite the syringe tip. Laminin was electrospun at 5% (w/v) in HFP, 12.5 cm collecting distance, 1.5 mL/h flow rate, and 20 kV driving voltage. After laminin collected on the coverslips, the samples were removed from the collector and placed into wells in a 24-well plate for cell culture.

Laminin films for cell culture were prepared on coverslips identical to those used for NF scaffold preparation as previously described.[26] Briefly, soluble laminin stock solution (sterile laminin, 3 mg/mL in tris-buffered saline—0.15 M Tris, 0.05 M NaCl [pH 7.5]) was diluted into either distilled water or 0.1 M ammonium carbonate (pH 7.8) to a final concentration of 10 μg/mL. Twenty microliters of the solution was evaporated overnight onto a sterile, glass coverslip 5 mm in diameter under a laminar flow hood, yielding 0.2 μg of dried laminin film covering the upper surface of each coverslip. Coverslips were then placed into wells in a 24-well plate for cell culture.

Hydration study

LNF meshes were electrospun onto coverslips as described above. Meshes were placed in 24-well-plate dishes and immersed in 500 μL Dulbecco's modified Eagle's medium (DMEM) plus antibiotics to maintain similarity to ASC and PC12 culture conditions. Meshes were incubated at 37°C for 30 min, 6 h, or 24 h. At each time point, a group of three LNF meshes were removed from incubation, aspirated, and dried in vacuum desiccators overnight. Dried samples were mounted on aluminum mounts with carbon adhesive, coated with gold, and imaged using a JEOL 6400 SEM with Orion image processing. Fiber diameters were measured as described above.

Cell isolation and culture

Adipose tissue was obtained through the Department of Plastic Surgery at the University of Virginia in compliance with the UVa Human Investigation Committee. ASCs were isolated from the lipoaspirate using previously described methods.[27] Cells were grown in culture medium consisting of DMEM, 10% fetal bovine serum, and 1% antibiotic/antimycotic. The cells were initially plated ($p = 0$) and maintained at 37°C with 5% CO_2. Subconfluently, cells were released with 0.5% trypsin/EDTA and then either replated at 2000 cells/cm^2 or used for experiments. For serum-free culture, DMEM plus 1% antibiotic/antimycotic was used.

Cell attachment assay

ASC attachment was compared on LNFs and laminin films. ASCs were chosen as a promising source for nerve tissue engineering applications. Cells were dispersed using trypsin, and the reaction was stopped with soybean trypsin inhibitor. After counting, cells were plated in triplicate using an initial seeding density of 8×10^4 cells/cm^2 (15,000 cells per coverslip) onto coverslips coated with either laminin films or NFs. Substrates were placed in the incubator (37°C; 5% CO_2), and cells were allowed to attach for 15, 30, 60, or 120 min in serum-free DMEM, after which time they were washed from the substrates using Hank's balanced salt solution and fixed using 4% paraformaldehyde. Serum-free medium was used to prevent serum proteins from enhancing attachment, requiring cells to utilize the laminin substrate or secrete their own matrix proteins in response to the substrate. Substrates were imaged on a Hoffman Optics inverted light microscope at 4×, and cells were counted in Image J. Some ASCs were maintained in culture conditions for 3 days and then analyzed by scanning electron microscopy.

ASC neurite extension assay

ASCs have been shown to differentiate into a nerve-like phenotype,[28] making them ideal cells to test laminin bioactivity. The induction of ASCs to nerve-like cell morphology was conducted on LNFs and films. ASCs were seeded in triplicate at an initial seeding density of 10^4 cells per coverslip (9000 cells/cm^2) on either laminin film or NF substrates. Cells were cultured for 24 h in serum-free commercially available media (UltraCulture). Briefly, cells were fixed using 4% paraformaldehyde for 15 min, then rinsed with phosphate-buffered solution (PBS). Cells were permeabilized with 0.4% Triton in PBS for 5 min, then rinsed and blocked in 2% goat serum in PBS for 15 min. Samples were rinsed with PBS and incubated with the primary antibody β-3-tubulin (1:200) in 2% goat serum in PBS for 1 h. Samples were rinsed with PBS and incubated with the secondary antibody for fluorescein isothiocyanate (FITC) (1:200) in PBS for 2 h. Cells were rinsed and mounted for imaging. Cells were imaged at 20× on a Nikon microscope with Hoffman Modulation Optics. Neuron-like cells were determined to be cells with round cell bodies and one or more extended processes. These were counted on each sample to yield total number and percent of neuron-like cells. The β-3-tubulin antibody was a gift from Anthony Frankfurter.

PC12 neurite extension assay

A neurite extension assay was performed using PC12 cells, a cell type known to extend neurites in response to NGF stimulation. Cells were seeded in triplicate on LNF substrates subconfluently at a density of 2.5×10^4 cells/cm^2 to allow sufficient space for process formation. Serum-free medium was

Table 1. Fiber Morphology Values Measured from Scanning Electron Micrographs Using Image J

	Concentration (w/v)		
	3%	5%	8%
Diameter (nm)	112.85	143.36	222.87
Standard error	23.60	21.36	41.92
Bead area density (%)	18.80	9.63	3.43
Standard error	1.02	0.77	0.94

	Flow rate (mL/h)			
	0.5	1.5	2	3
Diameter (nm)	132.34	154.97	161.62	175.15
Standard error	19.23	30.17	28.32	24.29
Bead area density (%)	9.70	10.28	10.99	11.50
Standard error	0.56	0.99	0.97	0.55

	Distance (cm)			
	12.5	25	Concentration (w/v)[a]	p-value
Diameter (nm)	99.57	126.14	3%	0.323
Standard error	19.26	13.65		
Bead area density (%)	15.01	23.85		0.047
Standard error	0.35	0.96		
Diameter (nm)	141.06	152.56	5%	0.225
Standard error	19.70	8.27		
Bead area density (%)	8.04	15.99		0.007
Standard error	0.62	0.47		
Diameter (nm)	203.57	280.78	8%	0.003
Standard error	34.27	24.15		
Bead area density (%)	3.83	2.23		0.386
Standard error	0.90	0.27		

Data are presented by parameter; for example, concentration table contains all fibers spun at the recorded initial concentrations, regardless of flow rate or collecting distance.

[a]Student's *t*-test performed on two distance groups within a concentration to give *p*-value indicated in table.

used to prevent serum proteins from enhancing neurite extension and to illustrate the effect of the substrate specifically on neurite extension. NGF was added up to 50 ng/mL to the NGF-stimulated group after 2 h. Half the medium was changed for each sample after 48 h. After 5 days in culture, cells were rinsed in PBS and then fixed in 4% paraformaldehyde for 120 min at 4°C. Following fixation, cells were imaged using a Nikon TE 2000-E2 confocal microscope. Representative images were acquired using a 60×/1.45 Nikon oil immersion objective and MicroFire Picture Frame imaging software (Optronics, Galeta, CA). Processes were established to be any cellular extension longer than the diameter of the cell; these were counted to determine number per cell. Concurrently, PC12 cells were grown and passaged on tissue culture plastic as a control.

Statistics

To compare NF hydrated diameters, a one-way ANOVA was performed with a Tukey's *post hoc* test using Minitab software. For the cell attachment assay and neurite extension assays (for both ASCs and PC12 cells), cell or neurite counts were input into Minitab software and paired Student's *t*-tests were performed to determine statistically significant differences between conditions. Student's *t*-tests were also used to determine significant differences in nerve-like ASC morphology. Significance for all statistical tests was asserted as $p < 0.05$. Histograms were plotted in Minitab for neurite extension comparisons.

Results

Parametric analysis

A parametric study was necessary to determine the effects of the physical parameters of electrospinning, specifically concentration, distance, and flow rate, on resultant laminin fiber morphology. To create a map of parameters needed to produce particular fiber morphologies, we chose the parameters within standard ranges for biological polymer electrospinning shown in Table 1 and performed trials with each of the parameter sets. Driving voltage was held constant throughout at 20 kV.[29] Representative scanning electron micrographs are shown in Figure 1.

Fiber diameter and bead area density were chosen as appropriate metrics to assess and compare morphologies among the parameter sets. Each parameter was taken as a separate set for visualization purposes; for example, all solutions electrospun using 3% (w/v) initial concentration are included in the group labeled 3%, regardless of the collecting distance or flow rate used. As seen in the micrographs and further supported by the data shown in Figure 2, fiber diameter increased linearly with initial solution concentration over both collecting

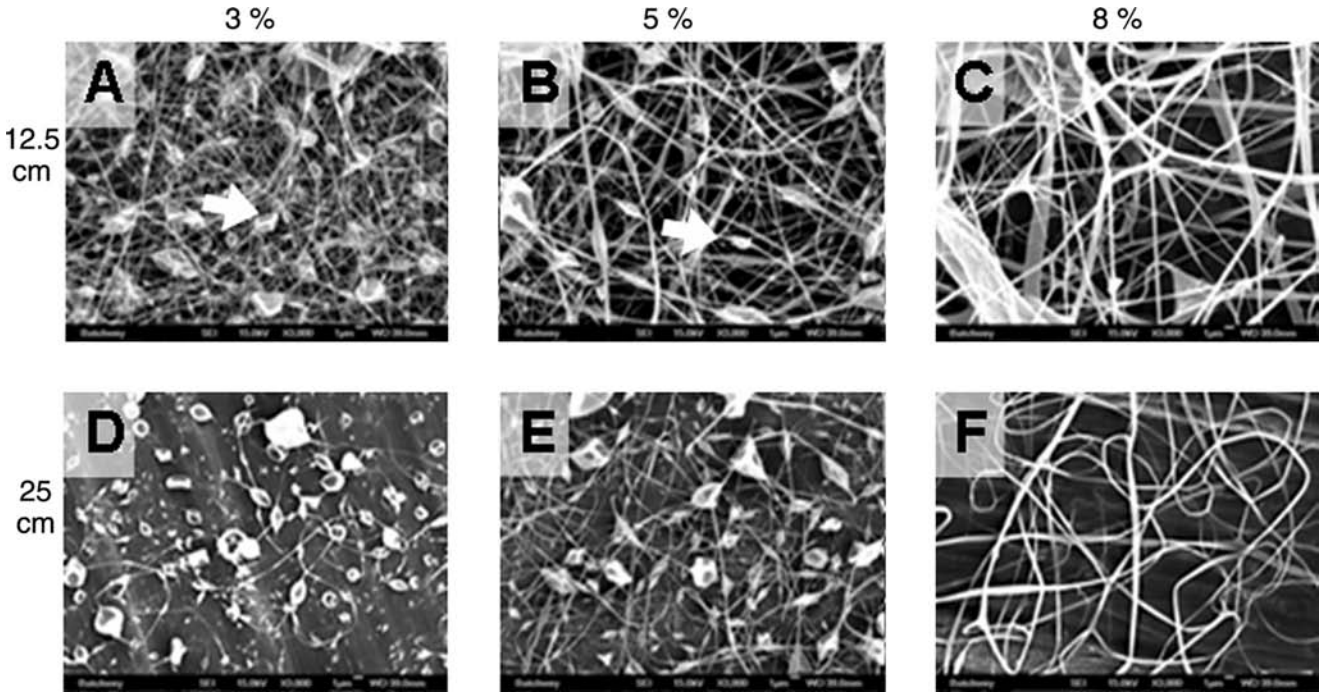

FIG. 1. Scanning electron micrographs of laminin electrospun at 20 kV driving voltage and 1.5 mL/h flow rate. Concentrations (w/v) in HFP are shown across the top, and collecting distance is shown along the left side. An increase in fiber diameter and decrease in bead area density are correlated with increasing percent laminin in HFP of the original solution. White arrows indicate matrisome morphology.

distances. Calculated linear regressions show an almost perfectly linear correlation ($R = 0.99$). Fiber diameter exhibits a less marked increase with increasing flow rate, although the linear correlation is equally strong ($R = 0.99$). The same trend emerges with working distance, with increasing collector distance translating to increased fiber diameter. We generated the smallest diameter fibers, 91.5 nm (±8.4 nm) average, with 3% (w/v) initial concentration, 1.5 mL/h flow rate, and 12.5-cm working distance. Overall, fiber diameter shows an approximate linear relationship to two of the physical parameters studied: concentration of initial solution and flow rate during electrospinning.

Although beads are a common product of the electrospinning process often regarded as defects, pioneering observations made by Martin *et al*. of the presence of the "matrisome" in basement membrane suggested that beaded structures may be important to the activity of authentic basement membranes.[30] Therefore, we measured bead area density to identify parameters that might control the area distribution of these matrisome-like structures. Representative images in Figure 1 (white arrows) show that several of the parameter sets used resulted in the matrisome morphology. Our data demonstrate a decreasing linear relationship between bead area density and initial solution concentration ($R = 0.97$), starting at 18.7% bead area density using the 3% (w/v) initial concentration and decreasing to only 3.4% bead area density with the 8% (w/v) initial concentration, as shown in Figure 2. However, increasing flow rate yields a linear increase in bead area density ($R = 0.98$). Under varying flow rates between 0.5 and 3.0 mL/h, we measured bead area densities ranging from 9.7% to 11.5%. Finally, no obvious trend emerged with the change in distance; instead, data again showed dependence on initial solution concentration. Over the two lower concentrations of 3% and 5% (w/v), we observed a statistically significant increase in bead area density of 15.0–23.8% and 8.0–16.0%, respectively, with increased collecting distance. When compared using a Student's *t*-test, these differences were statistically significant. With the higher initial concentration of 8% (w/v), the distances compared did not demonstrate statistically significant difference in bead area density, varying from 3.8% at the shorter distance to only 2.2% at the longer distance.

LNF hydrated morphology

For hydration studies, the median parameters were chosen to create the meshes, with the resulting morphology shown in Figure 1B. The parameter set chosen was an initial concentration of 5% laminin (w/v), flow rate of 1.5 mL/h, collecting distance of 12.5 cm, and the constant driving voltage of 20 kV that yielded a mean fiber diameter of 141.6 nm and 8.0% bead area density. Often, biological polymers, such as collagen, fibronectin, elastin, and others, require chemical crosslinking to maintain their morphology in culture. In the case of laminin, however, we have determined that no chemical crosslinking is necessary for laminin to retain its fibrous morphology in culture. As shown in Figure 3, laminin does not swell significantly in culture medium, even after 24 h at 37°C. Measured swelling of LNFs in aqueous media is consistently less than 10%, regardless of the amount of time the fibers are submerged. No statistically significant difference was found among the groups, including the control fibers that were not hydrated. This inherent property of LNFs to resist hydration in aqueous media makes them an attractive system to use

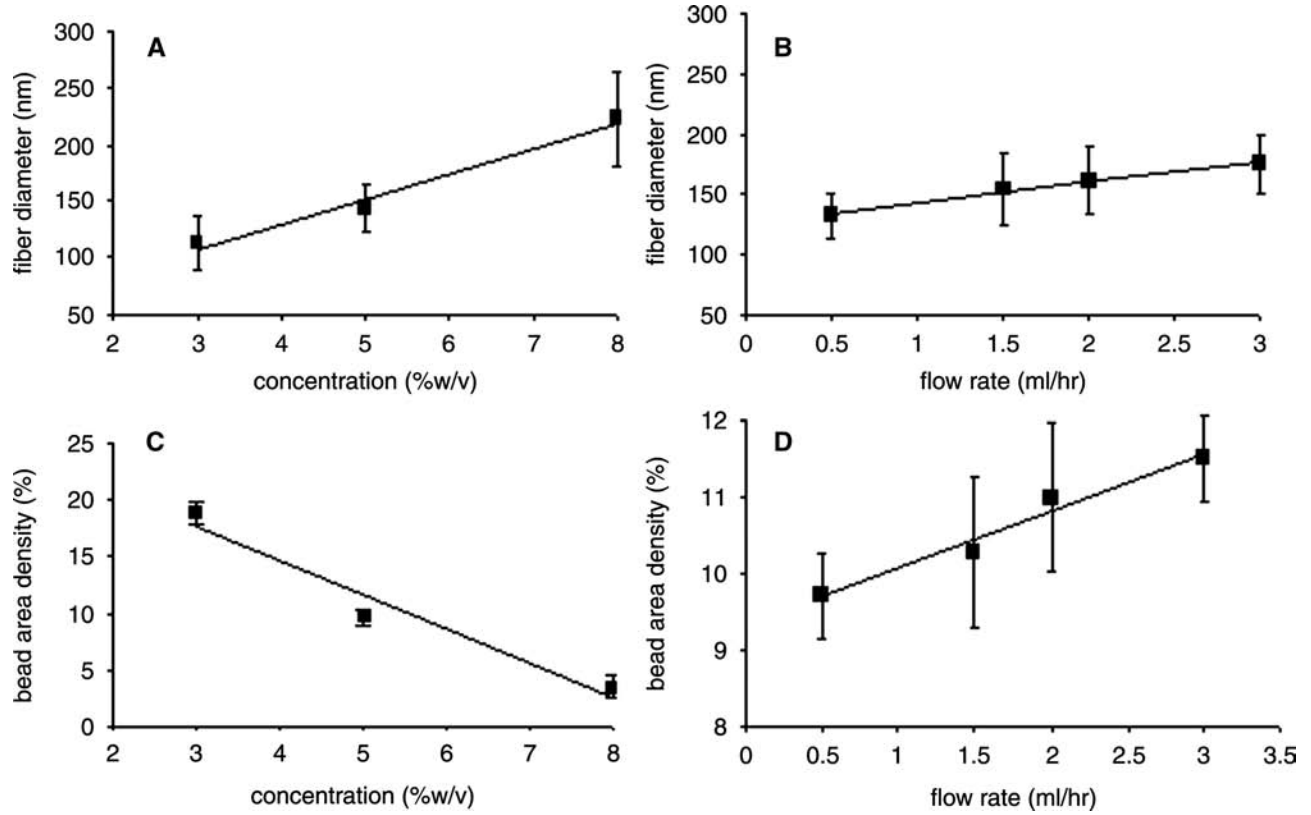

FIG. 2. Graphs displaying fiber diameter as a function of concentration (**A**) and flow rate (**B**). All solutions were spun at 20 kV driving voltage over two collecting distances (12.5 and 25 cm). Initial solution concentration is given as % w/v in HFP. Fiber diameter increases linearly with concentration (linear trendline $R = 0.991$) and flow rate (linear trendline $R = 0.988$). Graphs displaying bead area density as a function of concentration (**C**) and flow rate (**D**). Voltage was held constant over all trials at 20 kV. A strong linear relationship exists between bead area density and both concentration and flow rate, although concentration is inversely related (linear trendline $R = 0.975$) and flow rate is directly related to bead area density (linear trendline $R = 0.984$). Each group on the *x*-axis includes all parameter sets which contain that label, for example, 3% (w/v) concentration includes all NFs electrospun at 3% concentration, regardless of collecting distance or flow rate. Error bars display standard error measurements over the sample.

relative to other biological polymers, as no special processing is required to crosslink and reduce or remove residual chemical crosslinking agents.

Maintenance of bioactivity

After we achieved fibers of the desired morphology and tested their ability to maintain this morphology in culture medium, we investigated the attachment properties of the meshes using a potential neural progenitor cell. We examined the mesh as a substrate for ASCs, which have shown promise as a tissue engineering cell source. ASCs have been differentiated to a nerve-like phenotype[28] and have shown potential as a Schwann cell precursor,[31] making them a viable and appropriate cell source for peripheral nerve tissue engineering. To examine the compatibility of laminin for ASC attach-

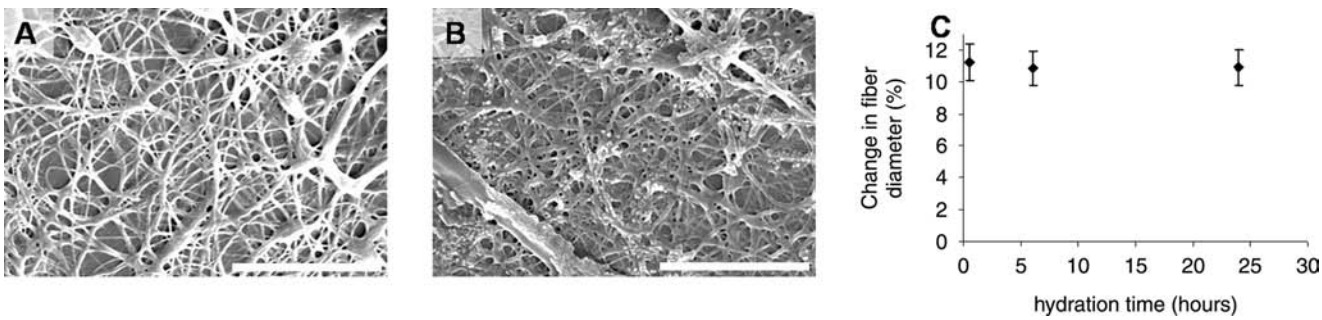

FIG. 3. Scanning electron micrographs of electrospun laminin after hydration in basal culture medium for (**A**) 30 min and (**B**) 24 h. Graph (**C**) illustrates change in fiber diameter of LNFs after hydration over 24 h. No significant difference was found across the timepoints.

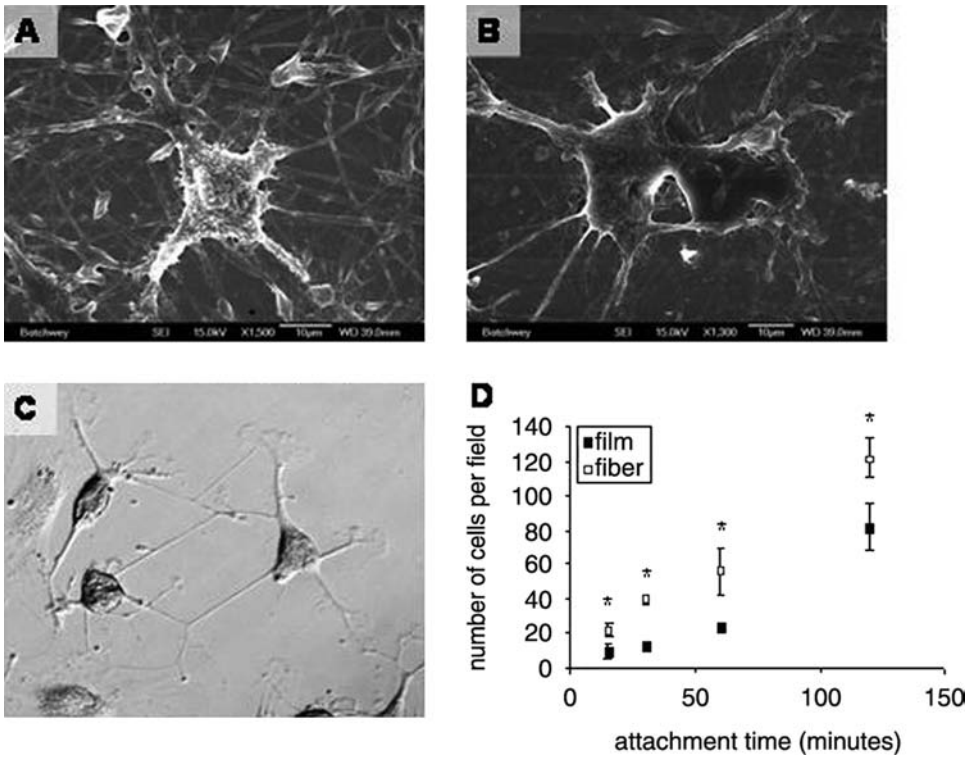

FIG. 4. (**A, B**) Scanning electron micrographs of ASCs on LNFs, and (**C**) light micrograph of ASCs differentiated into neuron-like cells in UltraCulture serum-free media on a laminin film, taken at 10× magnification. On the film, cells were stained for β-3-tubulin using the horse radish peroxidase (HRP) method. Observing the three neuron-like cells in the center, we see neurites formed as well as synapse-like structures between cells. In addition to nerve-like morphology, these cells show positive for β-3-tubulin as a nerve-specific marker. (**D**) Attachment assay to LNFs and laminin films. Cells were allowed to attach to the substrate for 15, 30, 60, or 120 min before being washed off, fixed, imaged, and counted using light microscopy and Image J processing techniques. Asterisks (*) indicate significantly greater attachment to fibers than films ($p < 0.05$).

ment, we performed a cell attachment assay comparing the attachment of ASCs on LNFs to laminin films. The assay was performed under serum-free conditions to exclude attachment mediated through serum proteins. Accordingly, the attachment measured was assumed to be mediated solely through the bioactivity of the substrate. Throughout the time course of the attachment study, cells showed significantly greater attachment to the NF substrate than the film substrate, as shown in Figure 4D. Because the cells attach more avidly to the NFs than equivalent saturating quantities of planar laminin, there are likely features related to size and scale of the NFs that are recognized by the cells.

Additionally, we have observed ASCs to acquire a neuron-like morphology and express β-3-tubulin, a nerve-specific marker, on laminin films, as shown in Figure 4C, extending neurite-like processes similar in morphology to dendrites and axons and forming cell–cell connections reminiscent of synapses. To determine whether LNFs would maintain and enhance this morphological change, we observed ASC attachment on LNFs and preferential process extension along fibers as shown in Figure 4A and B. To quantify this behavior, we observed ASC morphology after 24 h in UltraCulture, a commercially available serum-free media, on both LNFs and films. Cells that assumed a nervelike morphology by extending neurite-like processes as shown in Figure 5C and D were counted as a percent of total cells on each substrate. As in the attachment study, we observed a significantly higher number of neuron-like cells on the LNF substrates (Fig. 5B); however, when normalized with total cell number, the percent of ASCs assuming a nerve-like morphology was not significantly different (Fig. 5A).

To consider the cytocompatibility of LNFs for a nerve-like cell and to ensure that the bioactivity of laminin was maintained through processing, we investigated the response of PC12 cells to our laminin nanofibrous substrates. PC12 cells are a neuronal cell line derived from mouse pheochromocytoma and known to extend neurites in response to NGF. Additionally, PC12 cells have previously shown to extend neurites in response to a laminin substrate alone, without NGF stimulation.[32] We performed the neurite extension experiment on LNFs with and without NGF stimulation to determine if the laminin substrate alone would be sufficient for neurite extension. We observed that 78.99% of PC12 cells exposed to NGF extended neurites; surprisingly, when left unstimulated, a greater percentage (98.86%) of cells extended neurites. Figure 6 depicts number of neurites per cell and illustrates peak differences in number of cells per neurites. This representation shows not only the higher number of cells extending neurites in the unstimulated case, but also the right-skewed shape of the curve indicates that cells in the unstimulated case extended a higher number of neurites per cell. Both groups exhibited similar neurite extension, and while the mean neurite-per-cell measurement appears greater on NFs without stimulation, no statistically significant difference was found.

Discussion

Through the parametric study and subsequent hydration study, we were able to achieve nanoscale-diameter fibers that retained their fibrous morphology in culture medium without chemical crosslinking. The positive linear correlations we found between fiber diameter and initial solution concentration and flow rate are supported by previous research in the field. With synthetic polymers such as poly(lactide-co-glycolide)[33] and polycaprolactone,[34,35] and also other

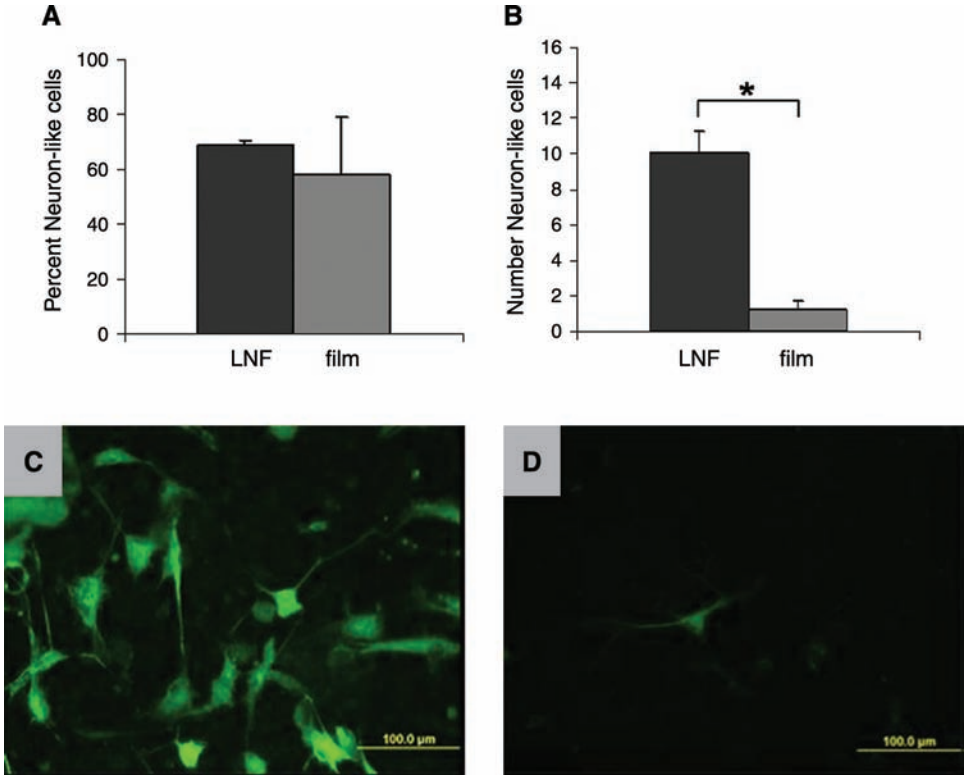

FIG. 5. (**A**) Percent of total ASCs exhibiting neuron-like morphology after 24 h in UltraCulture serum-free media on LNFs and laminin films. (**B**) Total number of ASCs exhibiting neuron-like morphology after 24 h in UltraCulture serum-free media. Error bars depict standard error. Representative fluorescence micrographs of ASCs immunohistochemically labeled for β-3-tubulin after 24 h in UltraCulture on (**C**) LNFs and (**D**) laminin film illustrate nerve-like cells. Asterisks (*) indicate significantly greater nerve-like cell numbers on LNFs than films ($p < 0.01$). Color images available online at www.liebertonline.com/ten.

biopolymers such as collagen[23] and elastin,[25] fiber diameter is generally observed to be smallest at the lowest solution concentration and flow rate, most likely due to limitations placed on the polymer content of the jet by these process parameters. Low flow rates (less than 1 mL/h) and low solution concentrations (dependent on polymer) cause less polymer to be ejected from the syringe needle toward the collector plate at any given time, leaving a greater volume of solvent to evaporate over a longer evaporation time and extending a small volume of polymer over a greater distance in space. Generally, as we strive to mimic basement membrane in our laminin nanofibrous scaffold, we will require a range of feature heights, widths, and porosities based on the particular native membrane we hope to recreate. The representation of diameter effects based on single parameters should be most useful in an experimental setting, guiding researchers with a particular fiber diameter in mind. As such, the relationships we have achieved through the parametric study should allow us to choose or alter specific physical parameters to create or adjust the fiber diameter and morphology we

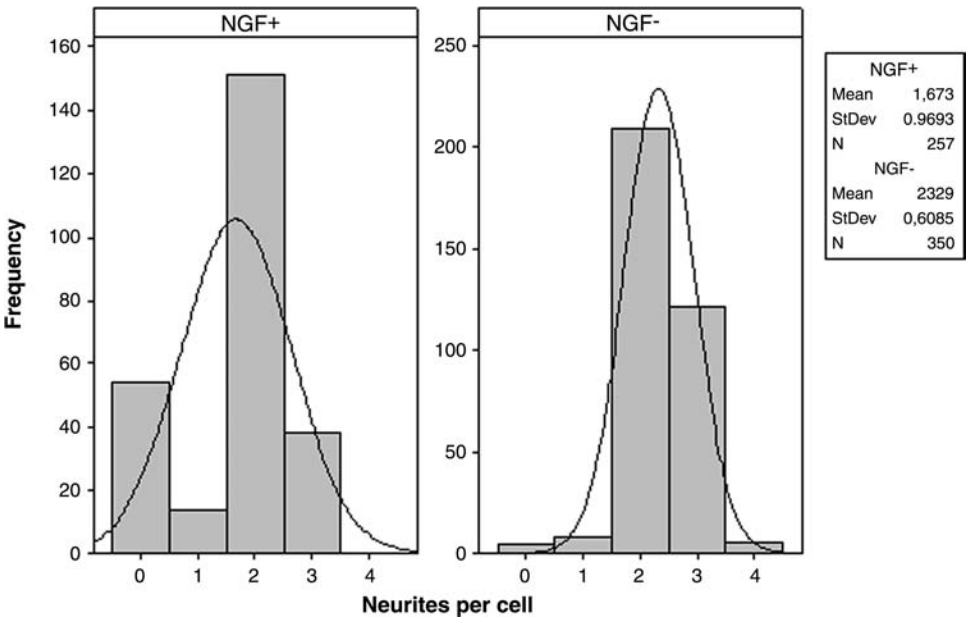

FIG. 6. Histogram depictions of neurites per cell for NGF-stimulated (NGF+) and unstimulated (NGF−) PC12 cells after 5 days in culture, along with descriptive statistics for each population.

desire, reducing the time and expense of trial and error in experimentation.

Additionally, the fibers generated show morphology characteristic of basement membrane. We achieve fiber diameters from 100 to 280 nm, solidly within the ranges shown by Flemming *et al*. for human corneal epithelial basement membrane feature sizes, and within the same order of magnitude as the laminin structures shown by Yurchenco and Ruben.[11,36] For example, as visible in Figure 1, electrospun laminin at lower concentrations forms structures reminiscent of matrisomes, structures composed of several basement membrane components such as type IV collagen, laminin, proteoglycans, and nidogen first discussed by Martin *et al*.[30] It has been suggested by their group that these tetrahedral structures are a primary site for cell attachment and direction of matrix synthesis and formation. The presence of similar structures in LNF meshes, and the observation that cells on a laminin matrix preferentially bind at these structures, supports the claim that laminin alone may provide a favorable substrate to provide cell attachment cues.

Laminin holds yet another advantage over other electrospun biological polymers such as collagens or fibrinogen: the ability to maintain fibrous morphology after exposure to an aqueous medium. Thus LNFs are the first reported protein NFs suitable for *in vitro* studies in which the protein is native. Based on diameter measurements before and after hydration, the meshes experience a slight swelling in aqueous media resulting in a less than 10% increase in fiber diameter. Similar collagen meshes show no fibrous morphology after hydration, yielding a structure more like that of a hydrated mat or gel than a fibrous mesh. The common solution to this issue is chemical crosslinking to assist fibers in retaining their shape upon hydration; however, crosslinking itself changes the fibrous morphology significantly, almost completely destroying the porosity of the mesh and causing flattening of fibers into a ribbon-like morphology, as observed by others.[17] Crosslinking of many proteins ablates biological activity, including laminin, which, when treated for sterilization by ultraviolet exposure, loses the ability to stimulate neurite extension of chick dorsal root ganglia.[37] It is possible that the process of electrospinning caused a change in the molecular structure of laminin, which, while maintaining biological activity, caused the LNFs to become insoluble in aqueous media. Notably, Kakade *et al*. have shown changes in the infrared spectrum of poly(ethylene oxide) suggestive of a change in the molecular structure of the fibers most likely resulting from a molecular level alignment of the individual polymer molecules.[38] In our system, this structural change caused by electrospinning may be the basis for the insolubility of LNFs in aqueous media; however, this may also result from loss of water solubility as a consequence of lyophilization of the laminin preparation before dissolution in the electrospinning solvent. Laminin is essentially insoluble in aqueous, physiological buffers following lyophilization, which is a process avoided in purification of laminin for that reason.[22] Additionally, Zeugolis *et al*. suggest that fluoroalcohols such as HFP cause protein denaturation, essentially unfolding collagen into gelatin and causing the solubility of collagen NFs in aqueous media.[19] The authors suggest that the denaturation of collagen to gelatin disrupts the triple-helical structure of the molecule. If this is indeed the case for collagen, a similar situation may exist with laminin. Laminin has a structure similar to collagen where the long arm (A chain) and short arms (B chains) wrap down to the globular domain at the carboxyl terminus of the A chain. Neuroactive sequences identified in laminin have been localized to the E8 fragment, near and within the globular domain of the long arm,[39] specifically the IKVAV sequence,[40] suggesting that even if the coil were to unwrap into its three component pieces with solubilization in HFP, the active region would remain intact on the long arm of the protein, maintaining the bioactivity we observed. Consequently, we have seen that laminin maintains its bioactivity after processing as demonstrated by our cell attachment and neuronal extension assay, suggesting either laminin resists denaturation by fluoroalcohols such as HFP, or maintains active regions intact through denaturation.

In the attachment assay, we have shown that laminin in either film or fibrous form is sufficient for ASC attachment under serum-free conditions. The LNF meshes, most likely due to their topography and physical similarity to basement membrane, facilitated ASC attachment over two-dimensional laminin films. Both LNFs and films induced ASCs to form neurite-like processes after 24-h exposure to the laminin substrate in serum-free media. In addition, significantly greater nerve-like cell numbers that attributed to greater cell attachment were seen in the LNF case, likely due to the nanostructure of the surfaces and higher surface area available for attachment than on two-dimensional films of the same substrate. Additionally, the extension of neurites by PC12 cells without standard NGF stimulation suggests that laminin retains its bioactivity even in NF form. PC12 cells are known to extend processes reversibly in the presence of NGF, achieving a nerve-like morphology, but cannot normally be forced to extend neurites without NGF by other means.[41] However, it has been shown that laminin can substitute for NGF stimulation to induce neurite outgrowth in these cells.[32] In our study, exposure to LNFs was sufficient to form processes, and NGF stimulation was unnecessary. In fact, no statistical difference was found between the stimulated and unstimulated cells, suggesting that the NFs substitute completely for the presence of NGF for neurite extension. Therefore, we have demonstrated that the ability of the substrate to promote neurite extension was not destroyed by any of our processing methods, specifically lyophilization, solubilization, and sterilization. This observation promotes LNF meshes as an ideal substrate for nervous system applications.

In conclusion, we have, for the first time, successfully electrospun laminin I using HFP as a solvent under varying process parameters. With the completion of the parametric study, we now have guidelines by which to select parameters to create varying fiber diameters and morphologies, allowing these parameters to be tailored to the design constraints of the particular tissue. Cells attach and grow on LNFs, and nerve-like cells extend processes without growth factor stimulation, making a nanofibrous laminin substrate ideal for many applications, particularly in nervous system tissue engineering.

Acknowledgments

The authors wish to thank Rebecca Ogle for her technical assistance in EHS tumor growth and laminin isolation. This study was supported by the National Science Foundation

Emerging Frontiers in Research and Innovation (EFRI) grant 736002 to Dr. Botchwey and the National Institute of Dental & Craniofacial Research grant DE-010369-08 to Dr. Ogle. Rebekah Neal is supported by the University of Virginia Biotechnology Training Program grant 5T32GM008715-08. Lauren Sefcik is supported by a National Science Foundation Graduate Research Fellowship.

Disclosure Statement

No competing financial interests exist.

References

1. Yurchenco, P.D., Amenta, P.S., and Patton, B.L. Basement membrane assembly, stability and activities observed through a developmental lens. Matrix Biol **22,** 521, 2004.
2. Hunter, D.D., Shah, V., Merlie, J.P., and Sanes, J.R. A laminin-like adhesive protein concentrated in the synaptic cleft of the neuromuscular junction. Nature **338,** 229, 1989.
3. Li, S., Harrison, D., Carbonetto, S., Fassler, R., Smyth, N., Edgar, D., and Yurchenco, P.D. Matrix assembly, regulation, and survival functions of laminin and its receptors in embryonic stem cell differentiation. J Cell Biol **157,** 1279, 2002.
4. Sonnenberg, A., Modderman, P.W., and Hogervorst, F. Laminin receptor on platelets is the integrin VLA-6. Nature (Lond) **336,** 487, 1988.
5. Colognato, H., Galvin, J., Wang, Z., Relucio, J., Nguyen, T., Harrison, D., Yurchenco, P.D., and Ffrench-Constant, C. Identification of dystroglycan as a second laminin receptor in oligodendrocytes, with a role in myelination. Development **134,** 1723, 2007.
6. Okazaki, I., Suzuki, N., Nishi, N., Utani, A., Matsuura, H., Shinkai, H., Yamashita, H., Kitagawa, Y., and Nomizu, M. Identification of biologically active sequences in the laminin alpha 4 chain G domain. J Biol Chem **277,** 37070, 2002.
7. Blum, J.L., Zeigler, M.E., and Wicha, M.S. Regulation of mammary differentiation by the extracellular matrix. Environ Health Perspect **80,** 71, 1989.
8. Clement, B., Segui-Real, B., Savagner, P., Kleinman, H.K., and Yamada, Y. Hepatocyte attachment to laminin is mediated through multiple receptors. J Cell Biol **110,** 185, 1990.
9. Yurchenco, P.D., Cheng, Y., and Colognato. H. Laminin forms an independent network in basement membranes. J Cell Biol **117,** 1119, 1992.
10. Tsiper, M.V., and Yurchenco, P.D. Laminin assembles into separate basement membrane and fibrillar matrices in Schwann cells. J Cell Sci **115,** 1005, 2002.
11. Flemming, R.G., Murphy, C.J., Abrams, G.A., Goodman, S.L., and Nealy, P.F. Effects of synthetic micro- and nano-structured surfaces on cell behavior. Biomaterials **20,** 573, 1999.
12. Abrams, G.A., Schaus, S.S., Goodman, S.L., Nealey, P.F., and Murphy, C.J. Nanoscale topography of the corneal epithelial basement membrane and Descemet's membrane of the human. Cornea **19,** 57, 2000.
13. Matthews, J.A., Wnek, G.E., Simpson, D.G., and Bowlin, G.L. Electrospinning of collagen nanofibers. Biomacromolecules **3,** 232, 2002.
14. Buttafoco, L., Kolkman, N.G., Engbers-Buijtenhuijs, P., Poot, A.A., Dijkstra, P.J., Vermes, I., and Feijen, J. Electrospinning of collagen and elastin for tissue engineering applications. Biomaterials **27,** 724, 2006.
15. Rogers, S.L., Letourneau, P.C., Palm, S.L., McCarthy, J., and Furcht, L.T. Neurite extension by peripheral and central nervous system neurons in response to substratum-bound fibronectin and laminin. Dev Biol **98,** 212, 1983.
16. Smith-Thomas, L.C., Fok-Seang, J., Stevens, J., Du, J.S., Muir, E., Faissner, A., Geller, H.M., Rogers, J.H., and Fawcett, J.W. An inhibitor of neurite outgrowth produced by astrocytes. J Cell Sci **107,** 1687, 1994.
17. Rho, K.S., Jeong, L., Lee, G., Seo, B.M., Park, Y.J., Hong, S.D., Roh, S., Cho, J.J., Park, W.H., and Min, B.M. Electrospinning of collagen nanofibers: effects on the behavior of normal human keratinocytes and early-stage wound healing. Biomaterials **27,** 1452, 2006.
18. Sheu, M.T., Huang, J.C., Yeh, G.C., and Ho, H.O. Characterization of collagen gel solutions and collagen matrices for cell culture. Biomaterials **22,** 1713, 2001.
19. Zeugolis, D.I., Khew, S.T., Yew, E.S., Ekaputra, A.K., Tong, Y.W., Yung, L.Y., Hutmacher, D.W., Sheppard, C., and Raghunath, M. Electro-spinning of pure collagen nano-fibres—just an expensive way to make gelatin? Biomaterials **29,** 2293, 2008.
20. van Wachem, P.B., van Luyn, M.J., Olde Damink, L.H., Dijkstra, P.J., Feijen, J., and Nieuwenhuis, P. Biocompatibility and tissue regenerating capacity of crosslinked dermal sheep collagen. J Biomed Mater Res **28,** 353, 1994.
21. Kleinman, H.K., McGarvey, M.L., Hassell, J.R., and Martin, G.R. Formation of a supramolecular complex is involved in the reconstitution of basement membrane components. Biochemistry **22,** 4969, 1983.
22. Kleinman, H.K., McGarvey, M.L., Liotta, L.A., Robey, P.G., Tryggvason, K., and Martin, G.R. Isolation and characterization of type IV procollagen, laminin and heparin sulfate proteoglycan from the EHS sarcoma. Biochemistry **21,** 6188, 1982.
23. Wnek, G.E., Carr, M., Simpson, D.G., and Bowlin, G.L. Electrospinning of nanofiber fibrinogen structures. Nano Lett **3,** 213, 2003.
24. Sefcik, L.S., Neal, R.A., Kaszuba, S.N., Parker, A.M., Katz, A.J., Ogle, R.C., and Botchwey, E.A. Collagen nanofibers are a biomimetic substrate for the serum free osteogenic differentiation of human adipose stem cells. J Tissue Eng Regen Med **2,** 210, 2008.
25. Buttafoco, L., Kolkman, N.G., Engbers-Buijtenhuijs, P., Poot, A.A., Dijkstra, P.J., Vermes, I., and Feijen, J. Electrospinning of collagen and elastin for tissue engineering applications. Biomaterials **27,** 724, 2006.
26. Kleinman, H.K., Ogle, R.C., Cannon, F.B., Little, C.D., Sweeney, T.M., and Luckenbill-Edds, L. Laminin receptors for neurite formation. Proc Natl Acad Sci USA **85,** 1282, 1988.
27. Zuk, P.A., Zhu, M., Mizuno, H., Huang, J., Futrell, J.W., Katz, A.J., Benhaim, P., Lorenz, H.P., and Hedrick, M.H. Multilineage cells from human adipose tissue: implications for cell-based therapies. Tissue Eng **7,** 211, 2001.
28. Kokai, L.E., Rubin, J.P., and Marra, K.G. The potential of adipose-derived adult stem cells as a source of neuronal progenitor cells. Plast Reconstr Surg **116,** 1453, 2005.
29. Katti, D.S., Robinson, K.W., Ko, F.K., and Laurencin, C.T. Bioresorbable nanofiber-based systems for wound healing and drug delivery: optimization of fabrication parameters. J Biomed Mater Res B Appl Biomater **70,** 286, 2004.
30. Martin, G.R., Kleinman, H.K., Terranova, V.P., Ledbetter, S., and Hassell, J.R. The regulation of basement membrane formation and cell-matrix interactions by defined supramolecular complexes. Ciba Found Symp **108,** 197, 1984.
31. Kingham, P.J., Kalbermatten, D.F., Mahay, D., Armstrong, S.J., Wiberg, M., and Terenghi, G. Adipose-derived stem

cells differentiate into a Schwann cell phenotype and promote neurite outgrowth *in vitro*. Exp Neurol **207,** 267, 2007.
32. Powell, S.K., Rao, J., Roque, E., Nomizu, M., Kuratomi, Y., Yamada, Y., and Kleinman, H.K. Neural cell response to multiple novel sites on laminin-1. J Neurosci Res **61,** 302, 2000.
33. Bashur, C.A., Dahlgren, L.A., and Goldstein, A.S. Effect of fiber diameter and orientation on fibroblast morphology and proliferation on electrospun poly(D,L-lactic-co-glycolic acid) meshes. Biomaterials **27,** 5681, 2006.
34. Thomas, V., Jose, M.V., Chowdhury, S., Sullivan, J.F., Dean, D.R., and Vohra, Y.K. Mechano-morphological studies of aligned nanofibrous scaffolds of polycaprolactone fabricated by electrospinning. J Biomater Sci Polym Ed **17,** 969, 2006.
35. Chen, Z.C., Ekaputra, A.K., Gauthamanm, K., Adaikan, P.G., Yu, H., and Hutmacher, D.W. *In vitro* and *in vivo* analysis of co-electrospun scaffolds made of medical grade poly(epsilon-caprolactone) and porcine collagen. J Biomater Sci Polym Ed **19,** 693, 2008.
36. Yurchenco, P.D., and Ruben, G.C. Basement membrane structure *in situ*: evidence for lateral associations in the type IV collagen network. J Cell Biol **105,** 2559, 1987.
37. Hammarback, J.A., Palm, S.L., Furcht, L.T., and Letourneau, P.C. Guidance of neurite outgrowth by pathways of substratum-adsorbed laminin. J Neurosci Res **13,** 213, 1985.
38. Kakade, M.V., Givens, S., Gardner, K., Lee, K.H., Chase, D.B., and Rabolt, J.F. Electric field induced orientation of polymer chains in macroscopically aligned electrospun polymer nanofibers. J Am Chem Soc **129,** 2777, 2007.
39. Edgar, D., Timpl, R., and Thoenen, H. Structural requirements for the stimulation of neurite outgrowth by two variants of laminin and their inhibition by antibodies. J Cell Biol **106,** 1299, 1988.
40. Tashiro, K., Sephel, G.C., Weeks, B., Sasaki, M., Martin, G.R., Kleinman, H.K., and Yamada, Y. A synthetic peptide containing the IKVAV sequence from the A chain of laminin mediates cell attachment, migration, and neurite outgrowth. J Biol Chem **264,** 16174, 1989.
41. Greene, L.A., and Tischler, A.S. Establishment of noradrenergic clonal line of rat adrenal pheochromocytoma cells which respond to nerve growth factor. Proc Natl Acad Sci USA **73,** 2424, 1976.

Address reprint requests to:
Edward A. Botchwey, Ph.D.
Department of Biomedical Engineering
University of Virginia
Box 800759, Health System
Charlottesville, VA 22908

E-mail: botchwey@virginia.edu

Received: November 5, 2007
Accepted: August 16, 2008
Online Publication Date: October 4, 2008